Constitutive modeling and inverse analysis of the flow stress evolution during high temperature compression of a new ZE20 magnesium alloy for extrusion applications

John E. Plumeri, Łukasz Madej, Wojciech Z. Misiolek

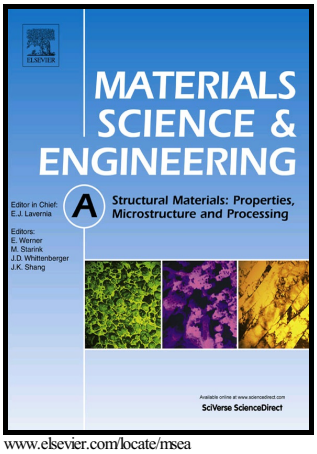

www.elsevier.com/locate/msea

PII: S0921-5093(18)31375-3
DOI: https://doi.org/10.1016/j.msea.2018.10.028
Reference: MSA37023

To appear in: *Materials Science & Engineering A*

Received date: 9 March 2018
Revised date: 4 October 2018
Accepted date: 5 October 2018

Cite this article as: John E. Plumeri, Łukasz Madej and Wojciech Z. Misiolek, Constitutive modeling and inverse analysis of the flow stress evolution during high temperature compression of a new ZE20 magnesium alloy for extrusion applications, *Materials Science & Engineering A*, https://doi.org/10.1016/j.msea.2018.10.028

Constitutive modeling and inverse analysis of the flow stress evolution during high temperature compression of a new ZE20 magnesium alloy for extrusion applications

John E. Plumeri[a], Łukasz Madej[b], and Wojciech Z. Misiolek[a]
[a]Loewy Institute, Lehigh University, Bethlehem, PA 18015, USA
[b]AGH University of Science and Technology, 30-059 Krakow, Poland

Keywords: Constitutive Modeling, Magnesium Alloys, Extrusion

Abstract
The high temperature deformation behavior of a new magnesium alloy, ZE20 (Mg-2.4%Zn-0.2%Ce), using uniaxial isothermal compression testing, is investigated within the paper. A set of experiments was conducted at temperatures of 350°C to 425°C, and strain rates in the range of 0.01 s^{-1} to 10 s^{-1}, and samples were compressed by 70% of their original length. An inverse analysis approach was used to evaluate flow stress curves based on load displacement measurements for each deformation condition. Flow stress evolution for the new alloy under these test conditions showed higher flow stress and lower work softening than commercially available magnesium casting alloys. Finally, constitutive equations predicting flow stress as a function of strain, strain rate, and temperature were applied to modeling mechanical response of the new alloy. Predictions from three constitutive models of steady state stress were validated against uniaxial compression data. It was found that all three models evaluated reliably predict the high strain stress values to within 15% of measured values.

1. Introduction

Magnesium is one of the least dense of structural alloys available to the engineering community. Its specific mechanical properties are excellent; its machinability, weldability, and thermal conductivity are all high. Pure magnesium's density is 1.7 g/cm^3, roughly a quarter that of iron and two thirds that of aluminum. For this reason, it has remained an important structural material for the aerospace industry for nearly a century, and represents a material with potential expansion of lightweight structural applications in a number of other industries such as the automotive sector. More widespread integration of magnesium alloys is hindered by a number of factors, however. Its corrosion resistance is poor, its cold formability is limited, and it exhibits a larger degree of mechanical anisotropy than other engineering alloys owing to its hexagonal crystallographic structure. However, the demand in industries such as transportation and personal electronics for extremely lightweight materials with excellent strength to weight ratios is an increasingly growing market, and hot forming technologies for magnesium components have been developed in recent years to improve wrought component mechanical properties while leveraging weight savings inherent to the alloys [1-4].

Extrusion has many benefits for processing a range of engineering profiles. Deformation above recrystallization temperatures allows for improved formability and mechanical properties in the finished profile compared with cast components. Extrudates exhibit very good surface finish and typically require few additional processing steps to yield a finished product, and the process can be adapted to produce large consistent lengths of a given profile while maintaining these advantageous finished properties.

For these reasons, hot extrusion of magnesium is an appealing technique for the production of structural sections. Grain structure and crystallographic texture influences the overall mechanical performance of the finished material. Texture randomization and grain refinement both improve performance of finished parts in wrought magnesium alloys. Deformation conditions, primarily temperature, strain, and strain rate, drive microstructural evolution during forming and, thus, the mechanical performance of the magnesium product. Finally, for the production of hollow profiles, the control of temperature and strain in the welding chamber are critical for the production of sound seam welds.

It has been recently demonstrated by Luo et al. that a novel magnesium-zinc-cerium alloy can be successfully extruded at elevated temperatures to produce finished components with improved ductility and more random texture compared with previously tested alloys. This alloy has composition Mg-2.4%Zn-0.2%Ce and is designated as ZE20. Table 1 shows the composition of this alloy as reported by [5].

Table 1. Chemical composition (weight%) of ZE20 magnesium alloy.

Al	Zn	Ce	Mn	Si	Fe	Cu	Ni
0.01	2.4	0.23	0.02	0.10	<0.005	<0.005	<0.003

Recent studies have assessed microstructural strengthening mechanisms that may contribute to the high ductility and favorable deformation behavior of this new alloy [6]. However, no efforts have been published to date investigating the constitutive behavior of this new alloy. The accurate prediction of the flow stress response of magnesium alloys across elevated strain, strain rate, and temperatures is thus of critical importance to the design process. Such predictions are crucial, as noted earlier, to the improvement of wrought magnesium alloy behavior [7].

Economical production of high performance magnesium extruded components requires the advanced prediction of material behavior in the high temperature compressive deformation regime characteristic of forming processes. Uniaxial compression tests, at a range of elevated temperatures and strain rates, are compared herein to constitutive equations for the description of flow stress evolution in the novel ZE20 magnesium alloy, for the purpose of obtaining an accurate prediction of material response and ultimate component performance in extrusion production.

2. Experimental materials and procedures

2.1 Uniaxial compression flow stress testing

It has been demonstrated that the dominant component of the state of stress driving plastic flow during extrusion processing is compression. It is thus necessary to obtain physical experimental compression data from the ZE20 alloy for the development of a constitutive model predicting flow stress evolution during extrusion processing.

Cylindrical test specimens 10 mm in diameter and 15 mm in length were machined via electrical discharge machining from as-cast ZE20 billets provided by the United States Automotive Materials Partnership (USAMP). Isothermal uniaxial compression tests were performed on a computer controlled Gleeble 3800 servohydraulic thermal mechanical testing machine. Specimens were heated to the testing temperature at 5 °C/s, soaked at test temperature for 3 min to ensure temperature uniformity, and compressed to 70% nominal strain. Strain rates of 0.01, 0.1, 1, and 10 s^{-1} were examined at temperatures of 350, 375, 400, and 425 °C. All specimens were water quenched within 20 seconds of mechanical testing.

2.2 Inverse analysis of flow stress data

Friction and adiabatic heating due to rapid plastic deformation in the test specimens contribute to the direct measurement of flow stress from the Gleeble instrumentation. To develop an accurate flow stress model for future prediction of deformation behavior, correction for the friction and deformation heating contributions to the flow stress data must be accounted for.

During the hot compression experiment, load and anvil displacement are directly measured by the Gleeble system. Research has shown that the most accurate and efficient method of calculating flow stress for the method of numerical modeling is by means of correcting the measured data via an inverse analysis [7]. The analysis effectively considers the influence of such factors as friction and deformation heating occurring during plastometric testing. The definition of the inverse problem has been described widely in literature; with regards to stress response as a function of strain it is given as:

$$\mathbf{d} = F(\mathbf{x}, \mathbf{p}), \quad F: R^k \rightarrow R^q \tag{1}$$

where $\mathbf{d} = \{d_1, \dots, d_q\}$ represents the vector of calculated values e.g. loads, $\mathbf{x} = \{x_1, \dots, x_l\}$ is the set of model parameters e.g. flow stress model coefficients, and $\mathbf{p} = \{p_1, \dots, p_k\}$ is the vector of process parameters e.g. strain rates, temperatures, etc.

The inverse analysis minimizes the value of the goal function. In the present paper the mean square root error between measured and calculated loads was used as a goal function. Figure 1 shows the measured and calculated loads for the compression test conditions. Figure 2 shows the corresponding true stress/strain data after inverse analysis for the same set of conditions. Stress and strain are calculated from load and stroke. It should be noted that the "calculated" lines correspond with corrected load values based on compensation for adiabatic deformation heating and friction contributions via the inverse analysis methods described above.

The flow stress models investigated in this study are thus based upon calculated flow stress data obtained from the inverse analysis, correcting for friction and deformation heating in the samples to reflect the true plastic deformation response of the material under compression loading.

2.3 Flow stress evolution observations

Figure 1 shows load curves as a function of displacement obtained from representative specimens during testing, after implementation of inverse analysis to mitigate the influence of friction between specimens and tooling, as well as adiabatic heating in the specimens due to plastic deformation. For the lower temperatures tested, ZE20 displays a period of moderate hardening after yielding until 30% strain. Compression specimens then reach a peak stress, and display limited work softening, which persists until high strains. The same behavior is seen for specimens tested at higher temperatures and moderate to high strain rates.

At higher temperatures and lower strain rates, ZE20 specimens do not exhibit the same hardening behavior. Instead, specimens exhibit hardening until about 40% strain, at which point they reach steady state behavior. This lack of softening could be due to the fact that these specimens are least likely to be affected by adiabatic heating [8]. Across all testing conditions, ZE20 specimens exhibit much less softening than is often reported for magnesium alloys. Magnesium alloys usually exhibit marked softening at intermediate strains, followed by steady-state behavior which is often attributed to dynamic recovery and recrystallization [9].

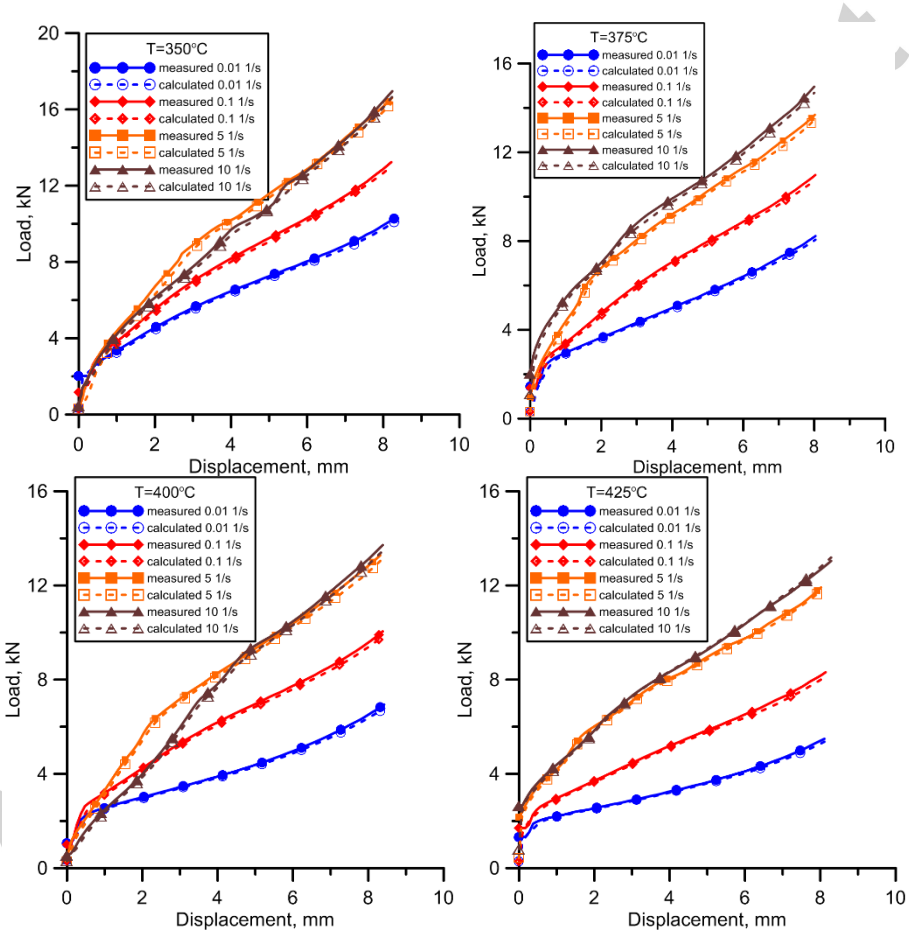

Figure 1. Measured raw load data and corrected loads from inverse analysis for different strain rates and temperatures.

3. Numerical model flow stress development

3.1 Model Preparation

Many flow stress models have been proposed in literature to describe the constitutive behavior of metallic alloys under varying deformation conditions. A wide array of physical, phenomenological, and empirical models has been variously applied to describe the flow stress evolution of various engineering alloys at varying process

conditions. One of each type of flow stress model was chosen to be evaluated for the quality of prediction of flow stress behavior of the new ZE20 alloy.

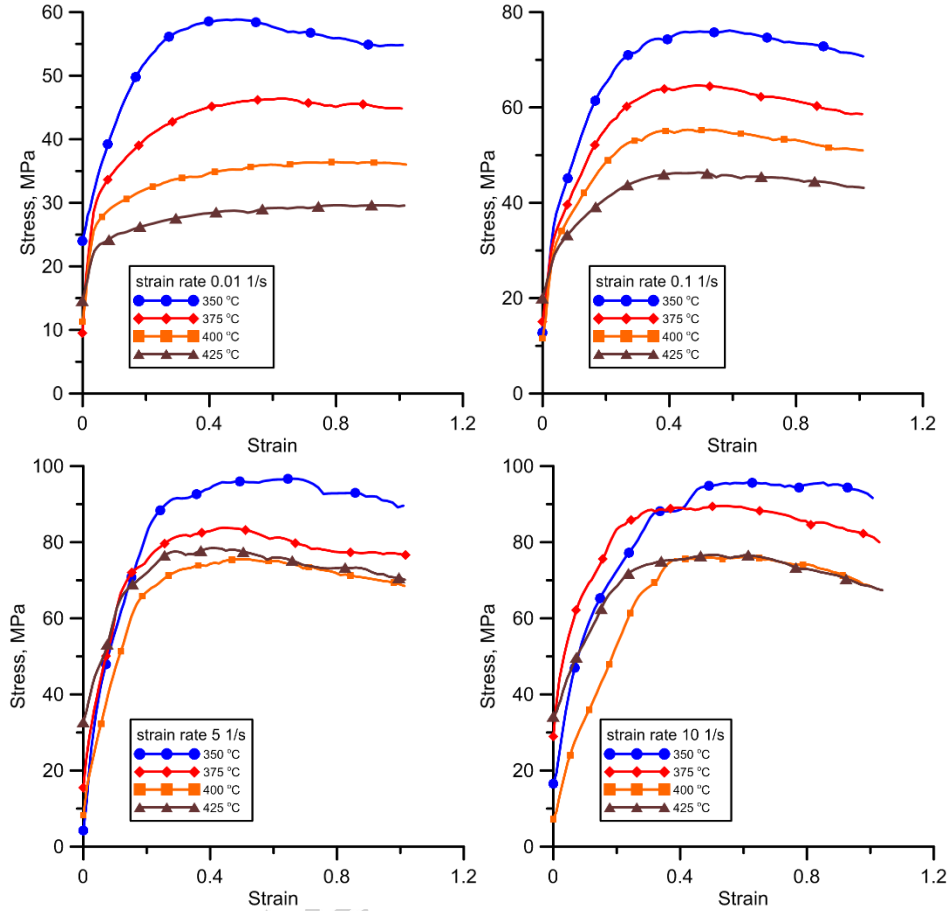

Figure 2. Stress/strain data after inverse analysis for variety of temperatures and strain rates.

A hyperbolic sine prediction with temperature-compensated strain rate, commonly known as the Zener-Hollomon parameter, is a phenomenological expression for peak or steady state flow stress. It is an ubiquitous model, which is used widely to predict deformation behavior in a wide range of metals and alloys over a wide thermal and mechanical range. A Johnson-Cook empirical model and a Zerilli-Armstrong physical model were also fit to the hot compression data and the quality of fit quantified. These three flow stress models were evaluated for the description of hot deformation behavior of the ZE20 alloy because of the variety of their bases and origin as well as their usefulness as demonstrated in literature to date.

3.2 Hyperbolic Sine-Arrhenius Model

The hyperbolic sine-Arrhenius type model is derived from creep phenomenological description [10]. The equation integrates the temperature compensated strain rate better known as the Zener-Hollomon parameter *Z*, as well as activation energy *Q*. The equations for flow stress and *Z* parameter are shown in Equations 2 and 3.

$$\sigma = \frac{1}{\alpha}\sinh^{-1}\left[\left(\frac{Z}{A}\right)^{1/n}\right] \quad (2)$$

$$Z = \dot{\varepsilon}e^{Q/RT} \quad (3)$$

The variables α, A, and n represent material constants, R is the universal gas constant, and Q is the activation energy for plastic deformation. Graphical methods were utilized for the fitting of constants for the Zener-Hollomon parameter, *Z*, otherwise known as temperature-compensated strain rate, as well as the hyperbolic sine

expression for flow stress in Eq.2. The procedure for this is extensively described in literature and, as such, only the pertinent plots will be detailed and parameters discussed in this study. Algebraic methods for obtaining the appropriate plots from the experimental data are described by Quan et al. [11], among many others.

It can be seen from Eq. 2 that the expression for flow stress does not include a strain term. The equation thus predicts a stress independent of strain, which is generally acceptable for the reason that high temperature deformation takes place. Because of the intended application of the ZE20 alloy is extrusion, and because the alloy is a lower ultimate strength material, its higher ductility, steady state stress was used as input for material constant calculation for the hyperbolic sine-Arrhenius equation. This steady state stress is defined here as the stress measured at maximum true strain reached in the experiment.

It is intended that the model predict stress at higher strains more accurately because of the large strains developed in deformation forming operations such as extrusion. As such the prediction of constitutive behavior at strains above 1.0, which is the limit of the compression test, is of interest in the present study. It should be noted that due to the mild strain softening across the thermomechanical range, peak stress prediction will have correspondingly low error with the material constants derived and presented here.

3.3 Johnson-Cook Model

The Johnson-Cook model is an empirically derived model which is also popular in literature. It is not mathematically complex and is versatile, having been used to model deformation at lower and higher temperatures for a wide range of materials, sometimes over very large strain and strain rate ranges.

The Johnson-Cook expression implemented in the current study is shown in Equation 4. The general form of the equation has been used here.

$$\sigma = (A + B\varepsilon^n)(1 + Cln(\dot{\varepsilon}^*))(D - ET^{*m}) \tag{4}$$

This equation includes the coefficients *A*, *B*, *C*, *D*, and *E*, as well as the exponents *n* and *m*. The homologous temperature, *T**, and the quasi-static strain rate $\dot{\varepsilon}_0$ are also included. Homologous temperature *T** is expressed as $T^* = (T - T_{room})/(T_{melt} - T_{room})$, where *T* is the temperature of the specimen, and $\dot{\varepsilon}^* = \dot{\varepsilon}/\dot{\varepsilon}_0$. The equation is a function of strain, strain rate, and temperature. Each of the three terms within the expression represents those three contributions respectively. Corresponding room and melting temperatures were taken to be 27 °C and 605 °C, respectively. The quasi-static strain rate is taken to be 0.1 s^{-1} in this study.

It can be seen that, by being a function of strain as well as strain rate and temperature, the Johnson-Cook equation is able to predict flow stress as a continuous function of strain [12]. A method of minimizing a total error function was applied based on iterative variation of equation constants *C*, *D*, *n*, and *m*. The goal function is a weighted quadratic error type as a function of predicted and experimental flow stress curves. Minimization of the sum of this function for all experimental data yielded the constants for the Johnson-Cook model. The goal function was weighted to prioritize stress prediction at strains above 0.5, yielding a flow stress model with greatest accuracy at higher strains and near steady-state stress values. The total error function *F* is a summation for all experiments expressed as

$$F = \sum \begin{cases} \sum_{i=1}^{n} \sqrt{\left(\sigma_{EXP,i} - \sigma_{CALC,i}\right)^2} & for\ \varepsilon \le 0.5 \\ \sum_{i=1}^{n} \sqrt{100\left(\sigma_{EXP,i} - \sigma_{CALC,i}\right)^2} & for\ \varepsilon > 0.5 \end{cases} \tag{5}$$

such that σ_{CALC} and σ_{EXP} are the predicted and measured stresses at discrete strain rate/temperature combinations, *i* is the data point, and *n* is the total number of data points collected via hot compression testing and compared with calculation based on the flow stress model predictions.

3.4 Zerilli-Armstrong Model

The Zerilli-Armstrong model is a physical model derived from dislocation mechanics. It is similar in mathematical form to the Johnson-Cook expression. The expression as implemented in this study is shown in Equation 5.

$$\sigma = C_0 + C_2\varepsilon^n e^{(C_3T + C_4Tln(\dot{\varepsilon}^*))} \quad (6)$$

In the same way that the Johnson-Cook model predicts a continuous flow stress as a function of strain, the Zerilli-Armstrong predicts constitutive behavior of alloys for strain, strain rate, and temperature. The terms $C_{0\text{-}4}$ are constants, n is the strain exponent [13], and the normalized strain rate is expressed as the same quotient as in the Johnson-Cook flow stress model. The value of the quasi-static strain rate is identical for both models.

The same method for equation constant optimization as used for the Johnson-Cook model was employed for the development of the material constants for the Zerilli-Armstrong model. A quadratic error function was implemented and iterative calculation used to minimize the predicted stress curves' error compared to experimental data. The same weighting scheme was also used so as to emphasize the strain prediction of the models and maximize accuracy at elevated steady state strain values above 0.5.

3.5 Constant Optimization

As described by the methods above, material constants for the three flow stress models were adapted to the ZE20 flow stress data for a range of strain rates at elevated temperatures. The experimental data set upon which these models are based spans the strain rates of 0.01-10 s^{-1} and temperatures of 350-425 °C. Table 2 shows the constants and the results of fitting operations for the respective flow stress models. Multiple coefficient sets could possibly be chosen for the given set of experimental conditions; however, a comparison of the numerical values of the coefficients to their physical meanings with regards to deformation behavior and material type as compared to literature has produced the values listed in the table.

Table 2. Constants for constitutive flow stress equations for the ZE20 alloy.

Hyperbolic sine-Arrhenius	
α (MPa^{-1})	0.018
n	10.7
A (s^{-1})	$4.96x10^{22}$
Q (kJ)	301
Johnson-Cook	
A (MPa)	68
B (MPa)	45
C	0.104
D	1.0
E	1.74
n	0.126
m	2.39
Zerilli-Armstrong	
C_0 (MPa)	10
C_2 (MPa)	27
C_3 (K^{-1})	0.0014
C_4 (K^{-1})	0.00016
n	0.08

4. Discussion

4.1 Microstructural Results

The completed compression tests were performed under typical industrial extrusion process conditions of temperature and strain rate and therefore allow for study of microstructural evolution corresponding to those in extruded profiles. Despite the selection of representative process parameters, gradients of strain, strain rate, and temperature are present in the compression samples as they are in the extrusion process. Analysis of the microstructure response to the extrusion process parameters is especially important for magnesium alloys known for

their strong anisotropy and bimodal grain size distribution. The grains in the cast billet (not pictured) showed a globular dendritic structure, with a grain size of 400 µm.

The selected light optical micrographs of compression test specimens are shown in Figure 3. Figure 3b shows a specimen after mechanical testing under different temperature and strain rate conditions. The microstructure response to deformation conditions of temperature of 350 °C and strain rate of 0.01 s^{-1} and at 425 °C and 10 s^{-1} is very different. In the case of lower temperature and lower strain rate, localized deformation in the form of a shear band is present (Figure 3a), while at higher temperature and higher strain rate more homogenous strain takes place (Figure 3b). The EBSD maps presented in Figure 4 are important in understanding the microstructure development. Maps in Figure 4 show that, at the same temperature of 350 °C, the higher strain rate of 10 s^{-1} compared to 0.01 s^{-1} resulted in much more fine grain microstructure, showing better refinement from the coarse cast grain microstructure. The lower strain rate resulted in nearly bimodal grain distribution, while the higher strain rate is dominated by fine grain microstructure.

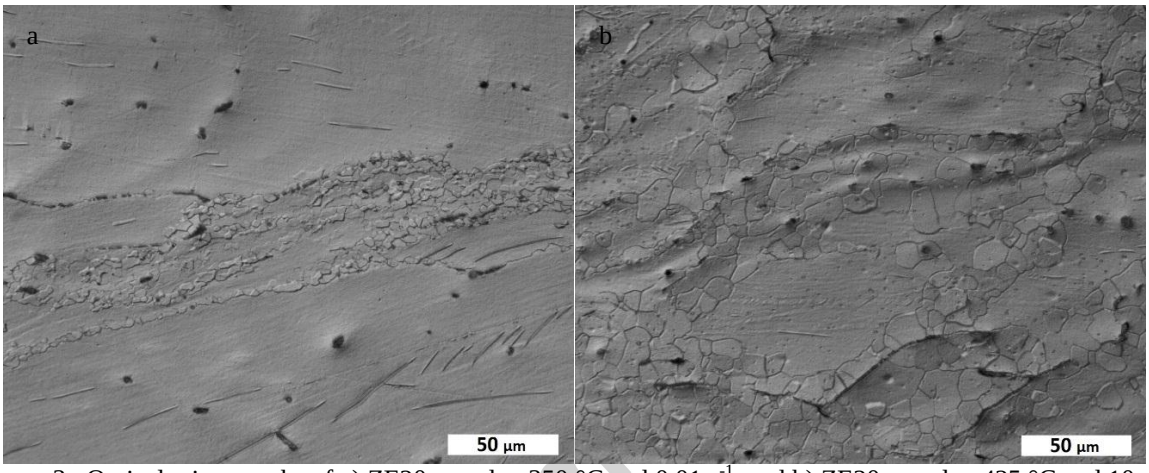

Figure 3. Optical micrographs of a) ZE20 tested at 350 °C and 0.01 s^{-1}, and b) ZE20 tested at 425 °C and 10 s^{-1}.

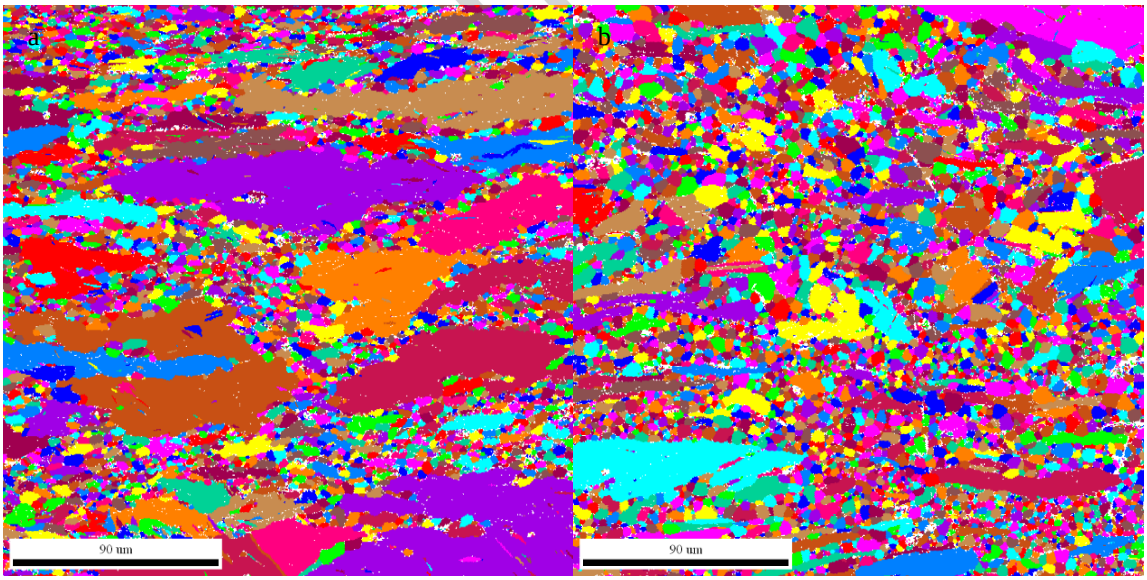

Figure 4. Electronic back scatter diffraction (EBSD) maps of compression specimens after testing at 350 °C with average strain rates of a) 0.01 s^{-1} and b) 10 s^{-1}.

4.2 Flow Stress Prediction

The comparison between mechanical response data and flow stress predictions from each of the three models is shown in Figure 5. The line marked "Ideal" represents the 1:1 slope of predicted vs. measured flow stress

or, in other words, the line at which the values of the predicted flow stress based on calculations from the various models is equal to the values of flow stress as measured from the compression tests, at high strain, quasi steady-state values of stress. Flow stress is calculated for the quasi-steady state condition at higher strains as measured by the stress and strain achieved at the end of the measured compression stroke. This stress was assumed to be the steady state value.

The data points presented in Figure 5 are reflective of the comparison between calculated and measured steady state flow stress values for the sixteen state points examined via hot compression testing. Namely, high true strain (ε = 1.0) quasi-steady state flow stress values for the combinations of strain rates of 0.01, 0.1, 1, and 10 s-1 as well as temperatures of 350, 375, 400, and 425 °C. The range of strain rate and temperatures for which the models are suitable is intended to be wide. It is assumed that stress predictions are valid for strain rates from quasi-static to high in the solid forming regime (approximately 0-10^2 s^{-1}). More importantly, deformation behavior at temperatures above 300 °C are meant to be predicted by the models, up to the onset of material melting point around 605 °C. As can be seen in the true stress-strain behavior of the ZE20 specimens from the uniaxial compression tests, only a small amount of softening is observed in the data. Thus, the flow stress predicted by the three models is able to balance capturing the peak levels of stress as well as the steady state approximation.

Examining the stress prediction trends of each of the three models, it can be seen that both the Johnson-Cook and the Zerilli-Armstrong models tend to over predict flow stress. This is most pronounced in the upper stress range corresponding with lower temperature and higher strain rate regimes. The hyperbolic sine-Arrhenius equation consistently under predicts the values of stress in this same region. At higher temperatures and lower strain rates, all three models closely predict measured stress values. Further, the higher temperature and lower strain rate flow stress response of this alloy shows little softening, and the shape of the stress curves predicted by the Johnson-Cook and Zerilli-Armstrong models are most accurate.

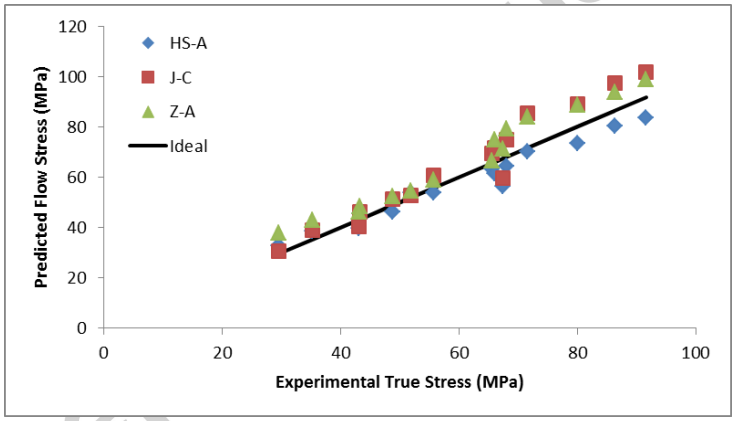

Figure 5. Predicted steady state flow stress as a function of measured true stress from the compression tests.

The hyperbolic sine-Arrhenius model predicts stress with less error across the temperature and strain rate range overall. It does not predict a full flow stress curve as a function of strain, however, so the accuracy of the predicted flow stress curve compared with experimental data cannot be evaluated in the same way as for the strain-dependent Johnson-Cook and Zerilli-Armstrong models. Though the two latter models tend to over-predict stress levels, especially in the higher stress regimes, they have the benefit of being calculated based on strain, strain rate, and temperature simultaneously. It is interesting to note that, though the mathematical formulation of both models is different, the flow stress predictions are very similar.

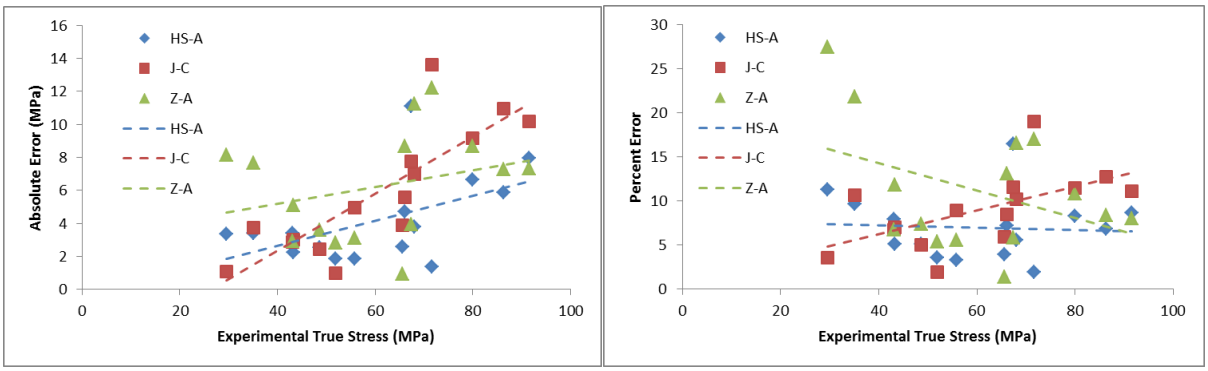

Figure 6. Predicted steady state stress from hyperbolic sine-Arrhenius, Johnson-Cook, and Zerilli-Armstrong constitutive models presented as a function of the measured true stress from experiments. Plots represent deviations as absolute stress and error as a percentage of the corresponding experimental steady state stress value.

Overall, for hot deformation processing of the new ZE20 alloy, particularly in the lower stress, higher temperature regime, all three constitutive models predict flow stress with great accuracy. Figure 6 shows a visualization of the running error predicted by each model. Up to approximately 70 MPa, the maximum deviation from experimental stresses is 17% for any of the three models. This occurs at 0.01 s^{-1} and 425 °C with the Zerilli-Armstrong model prediction at steady state flow stress value of 28 MPa. Over this entire low-stress range (below 70 MPa, corresponding to low strain rates of 0.1 s^{-1} and below for all temperatures), average deviation from measured stress is 3.3 MPa. This equates to 7.1% of the average predicted stress in higher strain rate and high temperature points (stresses in the approximately 50-70 MPa range), for all three models, it is shown that the percent error from experimental is roughly 10%. For highest temperatures and lowest strain rates, the Johnson-Cook model prediction trends lowest, below 5%, in terms of absolute and percent errors.

In the stress range above 70 MPa, the average deviation of predicted from measured stress is 7.9 MPa. This represents 10% of the average true stress in the range corresponding with strain rates of 5-10 s^{-1} across all temperatures 350-425 °C. When evaluating the accuracy of fit of the three constitutive models to the flow stress over the entire data set, across the entire stress range, the hyperbolic sine, Johnson-Cook, and Zerilli-Armstrong predict flow stress with an average deviation from the average true stress of 6.9%, 9.6%, and 10.4%, respectively. Lower steady state stress equates to the higher temperature flow regime, where material thermal softening dominates over strain rate hardening. All models are able to more accurately predict flow stress in the relatively lower steady state stress / higher temperature regime due to the particular flow stress behavior of this unique ZE20 Mg alloy in which the higher temperature flow stress curves exhibit a marked plateau with minimal strain softening from the initial point of maximum stress achieved in plastic compression. The approximately 70 MPa point represents a change in response of this specific alloy and most likely has to do with microstructure response to temperature and strain rate driving deformation, the effects of which are shown to some extent in Figures 3 and 4. However, a comprehensive study on specific phenomena has not been performed and only have speculative assessments towards that conclusion at this point.

This result is especially important because it indicates the FEM models' greatest accuracy at high temperature and strain rate deformation, which have been shown to produce superior extrudate properties at production rates necessary for economical industrial extrusion of ZE20 profiles [16-18]. The ability to apply the developed material model into FEM numerical simulations of magnesium extrusion is very important. It will now be possible to predict the influence of process parameters on state variables in the deformation zone and link them with resulting metallurgical and mechanical properties of extruded ZE20 components via simulation prior to full scale industrial production.

5. Conclusions

The variation of flow stress for magnesium alloy ZE20 across a wide temperature and strain rate range has been shown as a function of true strain. Marked differences have been observed in the flow stress behavior of this new alloy as compared with other commercially available wrought alloys such as AZ31. Of particular note is the absence of recovery-driven flow softening at high strains, as is observed in commercial magnesium alloys. ZE20 also exhibits higher steady-state flow stresses than AZ31 at elevated temperatures tested in this study.

The exceptional compression flow stress behavior of the new ZE20 magnesium alloy, with its unique hardening and softening characteristics compared with previously developed commercial magnesium alloys, highlights the importance of developing unique constitutive models of the ZE20 alloy. It is likely that the overall density of recrystallization sites and fraction of recrystallization are still lower than those in more widely reported studies of finer-grained magnesium alloys, which explains the relative lack of recovery-driven softening observed here. Flow stress predictions based on the FEM model in the regime of lower steady state stress, corresponding to the highest temperature set of compression test results, reflect the highest level of accuracy for all models investigated.

Three constitutive models were employed to study their applicability to the prediction of flow stress evolution in this new alloy. These models are taken from literature; an empirical Johnson-Cook, phenomenological hyperbolic sine-Arrhenius type, and a physical Zerilli-Armstrong model were each applied to the experimental data. All three models predicted flow stress most accurately in the high temperature and lower strain rate ranges. Both Johnson-Cook and Zerilli-Armstrong models tended to over-predict stress values in the higher strain rate regime. The hyperbolic sine-Arrhenius model describes flow stress as a function is independent of strain, and thus predicts only a single stress state for a given temperature and strain rate condition. Both Johnson-Cook and Zerilli-Armstrong models are functions of strain, strain rate, and temperature. Additionally, the flow stress predictions from both models were similar, though error as a percentage of measured stress values was slightly lower for the Johnson-Cook function. Across the entire temperature and strain rate range experimentally tested, all three models predicted flow stress with an average deviation of no more than 15% of the average true stress values.

Acknowledgments and disclaimer

This material is based upon work supported by the Department of Energy, National Energy Technology Laboratory under Award Number No. DE-EE0005660. This paper was prepared as an account of work sponsored by an agency of the United States Government. Neither the United States Government nor any agency thereof, nor any of their employees, makes any warranty, express or implied, or assumes any legal liability or responsibility for the accuracy, completeness, or usefulness of any information, apparatus, product, or process disclosed, or represents that its use would not infringe privately owned rights. Reference herein to any specific commercial product, process, or service by trade name, trademark, manufacturer, or otherwise does not necessarily constitute or imply its endorsement, recommendation, or favoring by the United States Government or any agency thereof. The views and opinions of authors expressed herein do not necessarily state or reflect those of the United States Government or any agency thereof. Such support does not constitute an endorsement by the Department of Energy of the work or the views expressed herein. The Loewy Family Foundation, through the Loewy Professorship at Lehigh University, provides partial support for W. Z. Misiolek, while the contribution of L. Madej at AGH University of Science and Technology is partially supported within the statute research project 11.11.110.593. S. Sutton from Ohio State University performed hot compression testing and provided metallographic analysis.

Data availability

The raw data required to reproduce these findings are available to download from https://data.mendeley.com/datasets/z45d2t647t/. The processed data required to reproduce these findings are also available to download from the same link

.

References

[1] A.E. Tekkaya, et al., Metal forming beyond shaping: predicting and setting product properties, CIRP Ann. Manuf. Technol. 64 (2015) 629-653.
[2] M. Kleiner, M. Geiger, A. Klaus, Manufacturing of lightweight components by metal forming, CIRP Ann. Manuf. Technol. 52 (2003) 521-542.
[3] S.M. Fatemi-Varzaneh, A. Zarei-Hanzaki, H. Beladi, Dynamic recrystallization in AZ31 magnesium alloy, Mater. Sci. Eng.: A 456 (1–2) (2007) 52–57.
[4] C.Y. Wang, X.J. Wang, H. Chang, K. Wu, M.Y. Zheng, Processing maps for hot working of ZK60 magnesium alloy, Mater. Sci. Eng.: A 464 (1–2) (2007) 52–58.
[5] A.A. Luo, R. Mishra, A. Sachdev, High ductility magnesium-zinc-cerium alloys, Scr. Mater. 64 (2011) 410-413.
[6] R.K. Mishra, A.K. Gupta, P.R. Rao, A.K. Sachdev, A.M. Kumar, A.A. Luo, Influence of cerium on the texture and ductility of magnesium extrusions, Scr. Mater. 59 (5) (2008) 562–565.
[7] J. Gawad, R. Kuziak, L. Madej, D. Szeliga, M. Pietrzyk, Identification of rheological parameters on the basis of

various types of compression and tension tests, Steel Research International (2/3) (2005) 131-137.
[8] B.H. Lee, N.S. Reddy, J.T. Yeom, C.S. Lee, Flow softening behavior during high temperature deformation of AZ31Mg alloy, J. Mater. Process. Technol. 187–188 (2007) 766–769.
[9] F.J. Humphreys and M. Hatherly, Recrystallization and Related Annealing Phenomena, Elsevier, 2004.
[10] C.M. Sellars and W.J.M.G. Tegart, On the mechanism of hot deformation, Acta Metallurgica 14.9 (1966) 1136-1138.
[11] G.Z. Quan, Y. Shi, Y.X. Wang, B.S. Kang, T.W. Ku, W.J. Song, Constitutive modeling for the dynamic recrystallization evolution of AZ80 magnesium alloy based on stress–strain data, Mater. Sci. Eng.: A 528 (2011) 8051-8059.
[12] G. Johnson and W. Cook, Fracture characteristics of three metals subjected to various strains, strain rates, temperatures, and pressures, Eng. Fract. Mech. 21 (1985) 31-48.
[13] F.J. Zerilli and R.W. Armstrong, Dislocation-mechanics-based constitutive relations for material dynamics calculations, J. App. Phys. 61 (1987) 1816.
[14] D. Ponge and G. Gottstein, Necklace formation during dynamic recrystallization: mechanisms and impact on flow behavior, Acta Mater. 46 (1) (1998) 69–80.
[15] M.R. Barnett, Z. Keshavarz, A.G. Beer, D. Atwell, Influence of grain size on the compressive deformation of wrought Mg-3Al-1Zn, Acta Mater. 52 (17) (2004) 5093–5103.
[16] A.H. Alharthi and W.Z. Misiolek, Microstructure Characterization of Extrusion Welding in a Magnesium Alloy Extrudate, Metallogr. Microstruct. Anal. 2 (2013) 395–398, DOI 10.1007/s13632-013-0099-z.
[17] Plumeri, John E., Lukasz Madej, and Wojciech Z. Misiolek. "Development of extrusion technology for magnesium alloy ZE20." Procedia Engineering 207 (2017): 389-394.
[18] J.E. Plumeri and W.Z. Misiolek, Magnesium alloy ZE20 extrusion forming model development for the simulation and prediction of industrial forming processes, XXIV Conference on Computer Methods in Metals Technology, January15-18, 2017, Zakopane, Poland.